



HAL
open science

Thermoelastic properties and crystal structure of MgSiO₃ perovskite at lower mantle pressure and temperature conditions

G. Fiquet, A. Dewaele, D. Andrault, M. Kunz, T. Le Bihan

► **To cite this version:**

G. Fiquet, A. Dewaele, D. Andrault, M. Kunz, T. Le Bihan. Thermoelastic properties and crystal structure of MgSiO₃ perovskite at lower mantle pressure and temperature conditions. *Geophysical Research Letters*, 2000, 27, pp.21-24. 10.1029/1999GL008397 . insu-03596953

HAL Id: insu-03596953

<https://insu.hal.science/insu-03596953>

Submitted on 4 Mar 2022

HAL is a multi-disciplinary open access archive for the deposit and dissemination of scientific research documents, whether they are published or not. The documents may come from teaching and research institutions in France or abroad, or from public or private research centers.

L'archive ouverte pluridisciplinaire **HAL**, est destinée au dépôt et à la diffusion de documents scientifiques de niveau recherche, publiés ou non, émanant des établissements d'enseignement et de recherche français ou étrangers, des laboratoires publics ou privés.

Copyright

Thermoelastic properties and crystal structure of MgSiO₃ perovskite at lower mantle pressure and temperature conditions

G. Fiquet,^{1,2} A. Dewaele,¹ D. Andrault,³ M. Kunz⁴ and T. Le Bihan⁵

Abstract. A new synchrotron X-ray diffraction study of MgSiO₃ perovskite at high-pressure and high-temperature has been carried out in a laser-heated diamond-anvil cell to 94 GPa and temperatures above 2500 K. MgSiO₃ perovskite is shown to be stable in this P-T range and adopts an orthorhombic structure (space group *Pbnm*), thus ruling out any phase transition or decomposition to an assemblage of denser oxides. Structural refinements show an increase of the orthorhombic distortion with increasing pressure, counterbalanced by a decrease of this distortion at high temperature, as evidenced by the Si-O-Si angle evolution. In addition, thermoelastic parameters identified from this new pressure-volume-temperature data set indicate that a significant amount of magnesiowüstite is required to match PREM bulk modulus profile, thus making a pure perovskite lower mantle unlikely.

1. Introduction

Information required for interpretation of seismological models of the Earth includes P-V-T equation of state data under the wide range of P-T conditions prevailing in the mantle. A wealth of thermoelastic properties has thus been collected during the past few years on important mantle minerals, such as olivine and its high-pressure polymorphs, pyroxenes, garnets, ilmenite and stishovite. The study of the Earth's deep interior has made people focus on (Mg,Fe)SiO₃ perovskite and (Mg,Fe)O magnesiowüstite, considered to be the two main phases of the lower mantle. Bulk moduli (K_T) and pressure and temperature derivatives are being increasingly well constrained by synchrotron-based X-ray diffraction P-V-T studies [Fei *et al.*, 1992; Fiquet *et al.*, 1998; Funamori *et al.*, 1996; Mao *et al.*, 1991; Wang *et al.*, 1994]. Few studies, however, have been able to achieve P-V-T measurements on MgSiO₃ perovskite samples under the actual pressure and temperature conditions of the lower mantle. Fiquet *et al.* [1998] measured the unit-cell parameters of the silicate perovskite up to pressures of 57 GPa and temperatures in excess of 2500 K.

A new series of experiments recently allowed us to achieve X-ray diffraction measurements to 94 GPa at high temperature, which are reported here. These experiments give new constraints on the P-V-T equation of state of MgSiO₃ perovskite, as well as on the detailed high-pressure high-temperature structural behavior of this perovskite. These results will be discussed to address the following points: (1) the stability field

of MgSiO₃ perovskite, (2) the structure response to extreme pressure and temperature conditions, (3) the thermal equation of state of that compound and (4) the implications for the Earth's lower mantle composition.

2. Experimental

Angle-dispersive X-ray diffraction experiments were carried out at high pressure and temperature in a laser-heated diamond-anvil cell at the ID30 dedicated high-pressure beamline of the ESRF (Grenoble, France). A detailed description of the laser-heating and diamond-anvil cell experimental set-up can be found elsewhere [Fiquet *et al.*, 1996]. A doubly focused monochromatic X-ray beam was used at wavelengths set between 0.4 and 0.5 Å in association with imaging plates and the fast scan technique available on the high pressure beamline of the ESRF to collect data over a 2θ interval from 4 to 25° (see Andrault *et al.* [1997] or Fiquet *et al.* [1998] for details). Wavelength as well as sample-detector distance were calibrated against a Si standard and standards for absorption edges. X-rays were focused to a spot of about 10 x 15 μm FWHM on the sample and data collected at each temperature for 2 to 5 minutes.

MgSiO₃ perovskite samples were synthesized (1) from synthetic MgSiO₃ enstatite and (2) from synthetic MgSiO₃ glass, mixed with platinum powder and transformed at high pressure and high temperature into perovskite-type MgSiO₃. These starting materials were loaded cryogenically in argon, which was used as pressure transmitting medium, or compressed without any pressure transmitting medium for the experiments performed above 50 GPa. Samples were either heated with a stabilized TEM00 CO₂ laser ($\lambda = 10.6 \mu\text{m}$, model 57-1-28 W from Synrad) for experiments carried out in argon below 50 GPa or with a stabilized high-power multimode Nd:YAG laser ($\lambda = 1.06 \mu\text{m}$, model 118F/CW from Quantronix) for experiments carried out above 50 GPa. Re gaskets with holes 70-100 μm in

Table 1. Volume measurements of MgSiO₃ perovskite at various pressure and temperature conditions

T (K)	P (GPa)	V (Å ³)	T (K)	P (GPa)	V (Å ³)
298	46.88 (30)	140.827 (54)	298	75.06 (30)	132.728 (17)
298	50.94 (30)	139.810 (28)	298	75.62 (30)	132.788 (17)
298	53.63 (30)	139.269 (24)	298	40.03 (30)	143.442 (20)
298	53.46 (30)	139.307 (43)	298	42.17 (30)	142.588 (15)
298	85.70 (30)	130.097 (22)	298	39.44 (30)	143.328 (20)
298	90.17 (30)	129.303 (24)	298	40.66 (30)	143.255 (23)
298	90.57 (30)	129.292 (17)	2897	67.41 (45)	139.549 (26)
298	38.63 (30)	143.777 (19)	2963	67.23 (79)	139.783 (34)
298	45.38 (30)	141.332 (27)	1179	94.15 (51)	129.656 (14)
298	46.44 (30)	141.200 (25)	1763	46.87 (80)	144.414 (30)
298	80.57 (30)	131.651 (23)	1889	52.21 (46)	142.652 (18)
298	29.50 (30)	147.178 (15)	2372	54.14 (46)	142.176 (29)
298	31.57 (30)	146.567 (18)	1995	88.00 (46)	132.296 (21)
298	31.47 (30)	146.537 (12)	1380	91.82 (82)	130.768 (27)
298	85.32 (30)	130.266 (12)	1681	79.74 (87)	133.829 (11)
298	70.12 (30)	133.641 (08)	1603	81.81 (68)	133.160 (14)
298	71.50 (30)	133.598 (14)	1918	46.78 (80)	144.319 (26)
298	65.88 (30)	135.058 (19)	2199	46.98 (63)	145.408 (68)
298	67.94 (30)	134.801 (27)	1845	43.09 (112)	145.464 (48)

¹Laboratoire de Sciences de la Terre, Ecole Normale Supérieure de Lyon, Lyon, France

²Now at Laboratoire de Minéralogie et Cristallographie, Université Pierre et Marie Curie (Paris VI), Case 115, Tour 16, 2^{ème} étage, 4 Place Jussieu, 75252 Paris cedex 05 (e-mail: fiquet@lmcp.jussieu.fr)

³Département des Géomatériaux, Institut de Physique du Globe de Paris, Paris, France

⁴Laboratory of Crystallography, ETH Zentrum, Zuerich, Switzerland

⁵ESRF, Grenoble, France

Copyright 2000 by the American Geophysical Union.

Paper number 1999GL008397.

0094-8276/00/1999GL008397\$05.00

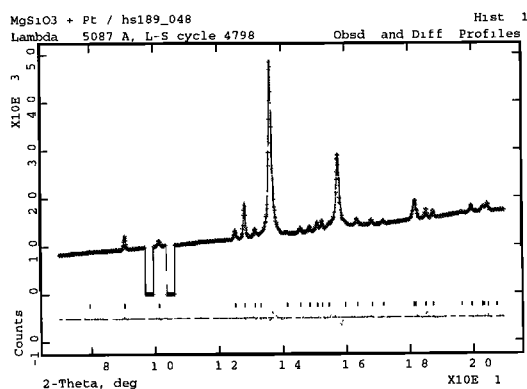


Figure 1. Integrated angle dispersive X-ray diffraction pattern collected at 79.7 GPa and 1681 K. Exposure time 5 minutes at wavelength $\lambda = 0.5087 \text{ \AA}$. Dashes, upper and lower solid lines represent experimental, calculated and difference spectra, respectively (see Table 2 for the details of refinement). Lower ticks: perovskite; upper ticks: platinum.

diameter were used. Temperatures were measured from the analysis of the sample thermal emission, collected every 5 seconds during the X-ray diffraction experiment with an optical set-up designed for this purpose [Fiquet *et al.*, 1996]. Because sample thickness was between 10 and 15 μm , we assume that the axial temperature gradient was negligible in such transparent samples. This assumption is supported by the experimental evidence of diffraction peak widths during laser-heating (0.05-0.08 degrees- 2θ) which are comparable to ambient conditions Si-standard (0.02-0.05 degrees 2θ). Pressures were inferred from the equation of state (EoS) of platinum [Jamieson *et al.*, 1982], used as an internal pressure calibrant. Temperature fluctuations recorded during the experiments have also been taken into account through the platinum P-V-T equation of state and appear in the pressure uncertainties reported in Table 1.

2-D images were integrated after spatial distortion and background corrections using program Fit2d [Hammersley, 1996] and treated using GSAS package [Larson and Von Dreele, 1988]. Le Bail profile refinements were applied to the diffraction patterns, in order to obtain reliable high-pressure high-temperature cell parameters for MgSiO₃ perovskite as well as for the pressure calibrant. In these experiments, a total of 20

Table 2. Refined unit-cell, atomic coordinates and selected interatomic distances (\AA) and angles (in degrees) for MgSiO₃ perovskite at 79.7 GPa and 1681 K.

Atom	x	y	z
Mg	0.5182(14)	0.5817(12)	$\frac{1}{4}$
Si	$\frac{1}{2}$	0	$\frac{1}{2}$
O(1)	0.1069(21)	0.4755(26)	$\frac{1}{4}$
O(2)	0.1883(16)	0.1939(16)	0.5621(13)
Bond distances			
Si-O(1) x2	1.686(3)	Mg-O(1) x1	1.894(11)
Si-O(2) x2	1.702(7)	Mg-O(1) x1	1.919(12)
Si-O(2) x2	1.703(8)	Mg-O(2) x2	1.922(8)
		Mg-O(2) x2	2.066(10)
		Mg-O(2) x2	2.275(10)
		Mg-O(1) x1	2.663(11)
		Mg-O(1) x1	2.882(12)
Mean <Si-O>	1.697	Mean <Mg-O>	2.188
Bond angles			
Si-O(1)-Si	146.3(6)	Si-O(2)-Si	142.2(5)

U_{150} not refined and fixed to the values of Ross and Hazen [1990]. The final discrepancy indices [Larson and Von Dreele, 1988] are $R_{wp} = 0.013$, $R_p = 0.007$, $R(\chi^2) = 0.070$ and reduced $\chi^2 = 0.151$. Space group: $Pbnm$, $Z=4$, $a = 4.4449(4) \text{ \AA}$, $b = 4.6648(4) \text{ \AA}$, $c = 6.4544(4) \text{ \AA}$, mixture composed of 86 wt% of MgSiO₃ perovskite and 14 wt% platinum.

reflections were used to refine the cell parameters of MgSiO₃ perovskite. Rietveld structural refinements were achieved on selected patterns at extreme pressure and temperature conditions, yielding detailed structural information on this compound (see Figure 1 and Table 2). In this last step, up to 24 parameters were adjusted for the background, the cell parameters of MgSiO₃ perovskite, platinum, or argon as well as two peak profiles for each compound, and atomic positions for the perovskite sample.

P-V-T data set was then fitted to a Birch-Murnaghan equation of state modified to take into account temperature effect on bulk modulus. We used a numerical code based on the generalized least squares inversion scheme of Tarantola and Valette [1982] to invert from the whole data set the ambient molar volume V_0 , the room-temperature bulk modulus K_0 , its first pressure derivative K'_0 as well as the first temperature derivative $(\partial K/\partial T)_P$, and the thermal expansion coefficients assuming an empirical expression $[\alpha = \alpha_0 + \alpha_1 T + \alpha_2 T^2]$. Alternatively, we used a Mie-Grüneisen equation of state to constrain the Grüneisen parameter γ and the q parameter (see Jackson [1998]).

3. Results and discussion

3.1. Stability field

Pressure-volume-temperature data are reported in Table 1. As shown in this table, diffraction patterns were recorded up to 94 GPa and almost 3000 K. In this pressure-temperature range, the patterns indicate that the $Pbnm$ orthorhombic structure is stable. We do not observe any phase transition or dissociation to an assemblage of perovskite and oxides, i.e. MgO and SiO₂, as observed by Meade *et al.* [1995] or Saxena *et al.* [1996]. This dissociation has been indeed observed above 65 GPa in the latter studies, which is in contradiction with our observations for at least five of our runs where orthorhombic perovskite was observed at pressures varying from 67 to 88 GPa combined with temperatures close to or exceeding 2000 K (see Figure 1 for example). On the other hand, our results confirm experiments carried out by Mao *et al.* [1997] who reported MgSiO₃ perovskite was stable to at least 80 GPa and by Serghiou *et al.* [1998], where perovskite was formed from oxides at pressures exceeding 100 GPa, both in laser-heated diamond-anvil cells. Furthermore, thermodynamic calculations show an extended pressure and temperature stability field for MgSiO₃ perovskite, when the denser high-pressure post-CaCl₂ structured SiO₂ polymorph reported by Dubrovinsky *et al.* [1997] is not taken into account [Matas *et al.*, in preparation]. Note however that this new silica phase is controversial since recent X-ray

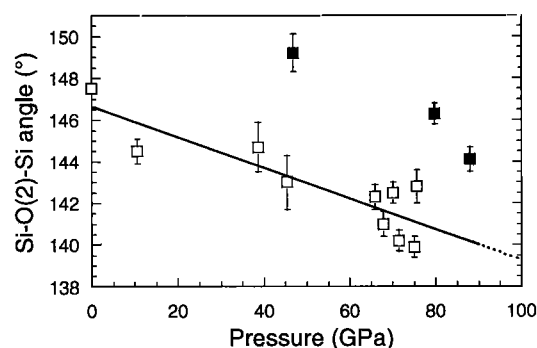


Figure 2. Measured tilt angle [Si-O(2)-Si] for MgSiO₃ perovskite as a function of pressure and temperature. The data points at room-pressure and 10 GPa are from Ross and Hazen [1990]. The increase of the orthorhombic distortion with increasing pressure, i.e. the decrease of the [Si-O-Si] angle, is obvious. The data collected at high-temperature (solid squares), on the other hand, show a decrease of this distortion.

diffraction experiments report the CaCl₂ structure of SiO₂ up to 120 GPa [Andraut *et al.*, 1998]. These results thus make the breakdown of perovskite to a denser assemblage of simple oxides very unlikely. The experimental observations of Meade *et al.* [1995] or Saxena *et al.* [1996] most likely originated in disequilibrium associated with large temperature gradients in the Nd-YAG laser-heating technique [e.g. Yagi *et al.*, 1997].

3.2. Structural evolution at high-pressure and high-temperature

The wide range of structural distortion away from the ideal cubic in perovskite-structured compounds had raised the possibility of pressure and/or temperature induced changes in the symmetry of (Mg,Fe)SiO₃ phases (see Wang *et al.* [1992]). Our new measurements demonstrate a wide P-T stability field for the Pbnm orthorhombic phase and a large compression anisotropy along *a*, *b*, *c* axes. The axial compressibilities calculated from least-squares fits of the compression data are $1.23 \times 10^{-3} \text{ GPa}^{-1}$, $0.98 \times 10^{-3} \text{ GPa}^{-1}$ and $1.21 \times 10^{-3} \text{ GPa}^{-1}$ for *a*, *b* and *c* axes respectively. This is in good agreement with results reported from a single crystal study by Ross and Hazen [1990] and compatible with an increase of the orthorhombic distortion with increasing pressure. Rietveld refinements done on selected patterns also yield detailed structural information on MgSiO₃ perovskite at high pressure and high temperature (see Table 2 and Figure 2). We observe, for instance, a clear trend in the evolution of the Si-O(2)-Si angle with pressure and temperature, with a significant decrease of the Si-O(2)-Si angle (i.e. increase of the orthorhombic distortion) with increasing pressure (Figure 2). On the other hand, we notice a decrease of this orthorhombic distortion mainly accommodated by a Si-O(2)-Si angle increase with increasing temperature at high pressure. In no case, however, was this angle variation large enough to come close to a tetragonal or cubic structure (i.e., Si-O-Si angles of 180°). The fact that the most important part of the distortion lies inside the Si-O-Si angle is well described (e.g. Sasaki *et al.* [1983]) and directly translates into the anisotropy in axial compression described above. In the same manner, the decrease of the orthorhombic distortion with increasing temperature observed even at high pressure agrees very well with the previous reports of Ross and Hazen [1989] and Parise *et al.* [1990], and shows that the behavior of MgSiO₃ perovskite with temperature mirrors its behavior under compression. Still, our measurements show that MgSiO₃ perovskite remains highly distorted under high-pressure conditions even at high temperature. The structural refinement results reported in Table 2 indeed yield a tolerance factor t_{obs} of 0.912 ($t_{\text{obs}}=1$ for an ideal cubic perovskite). It thus seems most likely that the Pbnm orthorhombic (Mg,Fe)SiO₃ perovskite phase remains stable relative to perovskites of higher symmetry along plausible lower mantle geotherms. Refinements carried out above 50 GPa also show that the assumption that SiO₆ octahedra are essentially rigid is questionable. Although most of the distortion with pressure is tilting of the octahedra, the degree of distortion and compression within the octahedra also changes under pressure or temperature. At around 70 GPa for instance, octahedra undergo almost 15% compression. Volume compression is thus also partly controlled by the shrinkage of Si-O bond lengths, which might take place at rather high pressures when the Si-O-Si tilting and thus the MgO₁₂ dodecahedron compression cannot be easily further increased.

3.3. Thermal equation of state

The room-temperature equation of state defined by the volume data recorded at room temperature after laser heating is in very good agreement with previous studies carried out under quasi-hydrostatic conditions, thus pointing out once again the efficiency of high-temperatures in releasing deviatoric stresses accumulated upon compression. The fit to a Birch-Murnaghan

Table 3. Parameters extracted from thermal equation of state for MgSiO₃ perovskite

Parameters	<i>A priori</i> parameters	(1)	(1)	(2)
V_0 (Å ³)	162.3 (fixed)	162.3	162.3	162.3
$K_{0,T}$ (GPa)	261	259	259.5 (9)	267.6 (9)
$K'_{0,T}$	4	3.7	3.69 (4)	3.78 (3)
$(\partial K/\partial T)_P$ (GPaK ⁻¹)	-0.02		-0.017 (2)	-0.021 (2)
α_0 (10 ⁻⁵ K ⁻¹)	2		2.18 (12)	1.54 (4)
α_1 (10 ⁻⁸ K ⁻²)	0.8		0.11 (8)	0.92 (9)
Θ_D	1100 K (fixed) [†]			
γ_0	1.4 [‡]			
q	1.4 (5)			

(1) optimized from data set presented in Table 1 and that of Fiquet *et al.* [1998], (2) optimized from data sets of Wang *et al.* [1994], Funamori *et al.* [1996] and Saxena *et al.* [1999]. 63 and 213 data points for data sets (1) and (2) respectively.

[†] Θ_D value from Anderson [1998]

[‡] preferred γ_0 value from the range of values calculated at room conditions by Jackson and Rigden [1996]

equation of state truncated to 3rd order yields a bulk modulus K_0 of 253(9) GPa, a pressure derivative $K'_0=3.9(2)$ and a room-pressure molar volume $V_0=162.27(1) \text{ Å}^3$. These results are in excellent agreement with the single crystal study of Ross and Hazen [1990] which yielded $K_0=254(13) \text{ GPa}$ with K'_0 fixed to 4, as well as with our previous study in which K_0 was found to be 256(7) GPa [Fiquet *et al.*, 1998]. This bulk modulus is also compatible with previous measurements to 30 GPa by Mao *et al.* [1991] who reported 261 GPa ($K'_0=4$).

Results of the inversion of the entire data set combined with that of Fiquet *et al.* [1998] are reported in Table 3. *A posteriori* errors on parameters were calculated from the resolution matrix assuming normally distributed errors and molar volume V_0 fixed to 162.3 Å³. A fit to a combination of data sets by Wang *et al.* [1994], Funamori *et al.* [1996] and Saxena *et al.* [1999] is included for comparison. From our new data, we obtained a $(\partial K/\partial T)_P$ value of -0.017(2) GPaK⁻¹. Although this value is slightly smaller than previous measurements found in the literature, i.e. $(\partial K/\partial T)_P=-0.020 \text{ GPaK}^{-1}$ [Utsumi *et al.*, 1995], -0.023(11) GPaK⁻¹ [Wang *et al.*, 1994], -0.027(5) GPaK⁻¹ [Fiquet *et al.*, 1998; Saxena *et al.*, 1999] and -0.028(17) GPaK⁻¹ [Funamori *et al.*, 1996], all these results almost agree within error bars. On the other hand, these results differ significantly from the extreme value of -0.063(5) GPaK⁻¹ reported by Mao *et al.* [1991].

The large pressure range explored in this study allows us to put strong constraints on the first pressure derivative of the incompressibility, which is lower than 4 ($K'_0=3.69$, see table 3). Surprisingly, a combination of all data is not efficient in constraining higher order terms such as $(\partial^2 K/\partial T^2)$, $(\partial^2 K/\partial P \partial T)$ and the α_2 term in the thermal expansion expression. Another frequently used thermal equation of state is the Debye Mie-Grüneisen equation of state (see [Fei *et al.*, 1992; Jackson, 1998]). As illustrated in Bina [1995], the trade-off between the q parameter $(\partial \ln \gamma / \partial \ln V)_T$ and the Grüneisen parameter γ_0 is not well constrained. As shown in Table 3, we obtain a value of 1.4 ± 0.5 for q when assuming a Grüneisen parameter γ_0 of 1.4, as obtained in the recent spectroscopic estimates of Gillet *et al.* [1996] and Jackson and Rigden [1996].

3.4. Geophysical implications

These new data on MgSiO₃ perovskite allow us to examine the effect of this material on constraining the composition of the lower mantle. With equation of state parameters listed Table 3, we calculate density and K_T for MgSiO₃ perovskite along a plausible lower mantle geotherm assuming a zero-depth foot temperature of 1830 K, which can be compared with density and K_T profiles calculated from PREM. The predicted density for a

pure (Mg,Fe)SiO₃ perovskite with 7% iron lower mantle is indistinguishable from PREM profiles. On the other hand, the K_T values are about 4-7 % higher than those predicted from the K_T profile of PREM, calculated after *Brown and Shankland* [1981]. About 10% (Mg,Fe)O is thus required to match the Earth's K_T profile under the hypothesis of a three-component lower mantle. Within the framework of a four components lower mantle [MgO, FeO, CaO and SiO₂], (Mg+Fe+Ca)/Si of 1.08(2) and Fe/(Fe+Mg)= 0.11(5) yield a density and bulk modulus that are consistent with those of PREM. In these calculations, the partitioning coefficient of iron between magnesiowüstite and perovskite was assumed to be constant and equal to 3 [e.g. *Martinez et al.*, 1997]. We assumed 8 vol% CaSiO₃ perovskite with thermoelastic parameters of *Wang et al.* [1996]. For magnesiowüstite, we used the P-V-T equation of state of *Fei et al.* [1992]. These results, although slightly different from those presented in *Fiquet et al.* [1998], make a pure perovskite lower mantle unlikely, in good agreement with conclusions drawn from previous experiments by *Wang et al.* [1994], *Funamori et al.* [1996], *Saxena et al.* [1999] or calculations by *Gillet et al.* [1996] or *Jackson and Rigden* [1996].

Still, a pure silicate perovskite lower mantle composition would also satisfy PREM density and bulk modulus profiles when the zero-depth foot temperature of the lower mantle adiabat is fixed to 2400 K instead of 1830 K. It must be also noted that no *in situ* experimental study has been for the moment able to clearly show the effect of iron substitution on the thermal equation of state of (Mg,Fe)SiO₃ perovskite. The shift in thermal expansivity with increasing iron content, however, seems to be rather small [*Anderson and Hama*, 1999]. Aluminium is also a very important component that has to be taken into account since the 4 or 5 mole percent of aluminium oxide (Al₂O₃) present for all proposed mantle compositions is believed to be incorporated into (Mg,Fe)SiO₃ perovskite [*Irifune et al.*, 1996]. Al₂O₃ has been shown to have a large influence onto the thermal equation of state [*Zhang and Weidner*, 1999]. In addition, other experimental studies on magnesiowüstite at lower mantle pressure and temperature conditions are needed for a better refinement of lower mantle compositional models.

Acknowledgments. We would like to thank the ECC (ESRF Extreme Conditions Consortium) for the loan of the multimode Nd-YAG infrared laser used in this study, as well as S. Bauchau for his help at the ID30 beamline. We thank J. Matas for the development of the inversion code and R.J. Hemley for his comments on the manuscript. Detailed and constructive reviews by C.R. Bina and J. Zhang are appreciated. This work has been possible under the auspices of INSU-CNRS Programme "Terre Profonde"

References

- Anderson, O.L., Thermoelastic properties of MgSiO₃ perovskite using the Debye approach, *Amer Mineral*, **83**, 23-25, 1998
- Anderson, O.L., and J. Hama, Shifts in thermal expansivity with Fe content for solid solutions of MgSiO₃-FeSiO₃ with the perovskite structure, *Amer Mineral*, **84**, 221-225, 1999
- Andraut, D., G. Fiquet, F. Guyot, and M. Hanfland, Pressure-induced Landau-type transition in stishovite, *Science*, **282**, 720-724, 1998
- Andraut, D., G. Fiquet, M. Kunz, F. Viscoekas, and D. Häusermann, The orthorhombic structure of iron an *in situ* study at high-temperature and high-pressure, *Science*, **278**, 831-834, 1997
- Bina, C.R., Confidence limits for silicate perovskite equations of state, *Phys. Chem Minerals*, **22**, 375-382, 1995.
- Brown, J.M., and T.J. Shankland, Thermodynamic parameters in the Earth as determined from seismic profiles, *Geophys. J. R. Astron. Soc.*, **66**, 579-596, 1981
- Dubrovinsky, L.S., S.K. Saxena, P. Lazor, R. Ahuja, O. Erkksson, J.M. Wills, and B. Johansson, Experimental and theoretical identification of a new high-pressure phase of silica, *Nature*, **388**, 362-365, 1997
- Fei, Y., H. Mao, and J. Hu, P-V-T equation of state of magnesiowüstite (Mg_{0.8}Fe_{0.4})O, *Phys. Chem. Minerals*, **18**, 416-422, 1992.
- Fiquet, G., D. Andraut, A. Dewaele, T. Charpin, M. Kunz, and D. Häusermann, P-V-T equation of state of MgSiO₃ perovskite, *Phys. Earth Planet. Int.*, **105**, 21-31, 1998
- Fiquet, G., D. Andraut, J.P. Itié, P. Gillet, and P. Richet, X-ray diffraction of periclase in a laser-heated diamond anvil cell, *Phys. Earth Planet. Int.*, **95**, 1-17, 1996.
- Funamori, N., T. Yagi, W. Utsumi, T. Kondo, T. Uchida, and M. Funamori, Thermoelastic properties of MgSiO₃ perovskite determined by *in situ* X ray observations up to 30 GPa and 2000 K, *J. Geophys. Res.-Solid Earth*, **101** (B4), 8257-8269, 1996.
- Gillet, P., F. Guyot, and Y. Wang, Microscopic anharmonicity and the equation of state of MgSiO₃-perovskite, *Geophys. Res. Lett.*, **23**, 3043-3046, 1996.
- Hammersley, J., Fit2d, *ESRF publication*, 1996
- Irifune, T., T. Koizumi, and J.I. Ando, An experimental study of the garnet-perovskite transformation in the system MgSiO₃-Mg₃Al₂Si₂O₁₂, *Phys. Earth Planet. Interiors*, **96** (2-3), 147-157, 1996.
- Jackson, I., Elasticity, composition and temperature of the Earth's lower mantle: a reappraisal, *Geophys. J. Int.*, **134**, 291-311, 1998
- Jackson, I., and S.M. Rigden, Analysis of P-V-T data Constraints on the thermoelastic properties of high-pressure minerals, *Phys. Earth Planet. Interiors*, **96** (2-3), 85-112, 1996.
- Jameson, J.C., J.N. Fritz, and M.H. Manghni, Pressure measurement at high temperature in X-ray diffraction studies: gold as a primary standard, in Akimoto, S., Manghni, M.H. (eds), *High Pressure Research in Geophysics*, Reidel, Boston, 1982
- Larson, A.C., and R.B. Von Dreele, GSAS manual, report LAUR 86-748, Los Alamos National Laboratory, 1988.
- Mao, H.K., R.J. Hemley, Y. Fei, J.F. Shu, L.C. Chen, A.P. Jephcoat, Y. Wu, and W.A. Bassett, Effect of pressure, temperature and composition on lattice parameters and density of (Mg,Fe)SiO₃-perovskite to 30 GPa, *J. Geophys. Res.*, **96**, 8069-8079, 1991
- Mao, H.K., G. Shen and R.J. Hemley, Multivariable dependence of Fe-Mg partitioning in the lower mantle, *Science*, **278**, 2098-2100, 1997
- Martinez, I., Y. Wang, F. Guyot, R.C. Liebermann and J.C. Doukhan, Microstructures and iron partitioning in (Mg,Fe)SiO₃ perovskite-(Mg,Fe) magnesiowüstite assemblages: an analytical transmission electron microscopy study, *J. Geophys. Res.*, **102**, B3, 5265-5280, 1997.
- Meade, C., H.K. Mao, and J. Hu, High-temperature phase transition and dissociation of (Mg,Fe)SiO₃ perovskite at lower mantle pressures, *Science*, **268**, 238, 1995.
- Parise, J.B., Y. Wang, A. Yeganeh-Haeri, D.E. Cox, and Y. Fei, Crystal structure and thermal expansion of (Mg,Fe)SiO₃ perovskite, *Geophys. Res. Lett.*, **17** (12), 2089-2092, 1990.
- Ross, N.L., and R.M. Hazen, Single crystal X-Ray diffraction study of MgSiO₃ perovskite from 77 to 400 K, *Phys. Chem. Miner.* (16), 415-420, 1989.
- Ross, N.L., and R.M. Hazen, High-pressure crystal chemistry of MgSiO₃ perovskite, *Phys. Chem. Miner.* (17), 4228-4237, 1990.
- Sasaki, S., C.T. Prewitt, and R.C. Liebermann, The crystal structure of CaGeO₃ perovskite and the crystal chemistry of the GdFeO₃-type perovskites, *Amer. Mineral.*, **68**, 1189-1198, 1983
- Saxena, S.K., L.S. Dubrovinsky, P. Lazor, Y. Cerenus, P. Haggkvist, M. Hanfland, and J. Hu, Stability of perovskite (MgSiO₃) in the Earth's mantle, *Science*, **274**, 1357-1359, 1996
- Saxena, S.K., L.S. Dubrovinsky, F. Tutti, and T. LeBihan, Equation of state of MgSiO₃ with the perovskite structure based on experimental measurements, *Amer. Mineral.*, **84**, 226-232, 1999.
- Serghou, G., A. Zerr, and R. Boehler, (Mg,Fe)SiO₃ perovskite stability under lower mantle conditions, *Science*, **280**, 2093-2095, 1998
- Tarantola, A. and B. Valette, Generalized nonlinear inverse problems solved using the least squares criterion, *Rev. Geophys.*, **20**, 219-232, 1982.
- Utsumi, W., N. Funamori, T. Yagi, E. Ito, T. Kikegawa, and O. Shimomura, Thermal expansivity of MgSiO₃ perovskite under high pressures up to 20 GPa, *Geophys. Res. Lett.*, **22** (9), 1005-1008, 1995
- Wang, Y., F. Guyot, and R.C. Liebermann, Electron microscopy of (Mg, Fe)SiO₃ perovskite: evidence for structural phase transitions and implications for the lower mantle, *J. Geophys. Res.*, **97** (B9), 12,327-12,347, 1992.
- Wang, Y.B., D.J. Weidner, and F. Guyot, Thermal equation of state of CaSiO₃ perovskite, *J. Geophys. Res.-Solid Earth*, **101** (B1), 661-672, 1996
- Wang, Y.B., D.J. Weidner, R.C. Liebermann, and Y.S. Zhao, P-V-T Equation of State of (Mg,Fe)SiO₃ Perovskite - Constraints on Composition of the Lower Mantle, *Phys. Earth Planet. Interiors*, **83** (1), 13-40, 1994
- Yagi, T., B. O'Neill, T. Kondo, N. Miyajima, and K. Fujino, Post-garnet high-pressure transition effect of heterogeneous laser heating and introduction of some new techniques, *Eur. J. Mineral.*, **9**, 301-310, 1997
- Zhang, J., and D.J. Weidner, Thermal equation of state of aluminum-enriched silicate perovskite, *Science*, **284**, 782-784, 1999.
- G. Fiquet and A. Dewaele, Laboratoire de Sciences de la Terre, ENS Lyon, 46 Allée d'Italie, 69364 Lyon cedex 07, France.
- D. Andraut, Département des Géomatériaux, IPG Paris, 4 Place Jussieu, 75252 Paris cedex 05, France.
- M. Kunz, Laboratory for Crystallography, ETH Zentrum, Sonneggstr. 5, CH-8092, Zuerich, Switzerland.
- T. Le Bihan, ID30 beamline, ESRF, BP220, 38043 Grenoble cedex, France

(Received July 7, 1999; revised October 25, 1999; accepted November 3, 1999.)